Multi-User OFDM Based on Braided Convolutional Codes

Lentmaier, Michael; Tavares, Marcos B.S.; Zigangirov, Kamil; Fettweis, Gerhard

Published in:
Lecture Notes in Electrical Engineering/Multi-Carrier Systems & Solutions 2009

DOI:
10.1007/978-90-481-2530-2_3

2009

MULTI-USER OFDM BASED ON BRAIDED CONVOLUTIONAL CODES

Michael Lentmaier, Marcos B.S. Tavares and Gerhard P. Fettweis
Vodafone Chair Mobile Communications Systems
Technische Universität Dresden
01062 Dresden, Germany
{michael.lentmaier, tavares, fettweis}@ifn.et.tu-dresden.de

Kamil Sh. Zigangirov
Department of Electrical Engineering
University of Notre Dame
Notre Dame, IN, 46556, USA
kzigangi@nd.edu

Abstract Braided convolutional codes (BCCs) form a class of iteratively decodable convolutional codes that are constructed from component convolutional codes. In braided code division multiple access (BCDMA), these very efficient error correcting codes are combined with a multiple access method and inherent interleaving for channel diversity exploitation into one single scheme. In this paper, we describe the BCDMA principle and present simulation results for a frequency selective Rayleigh fading channel. Results for bit interleaved coded modulation (BICM) based on turbo and LDPC codes are also given for comparison.

1. Introduction

There is a huge demand for higher data rates in next generation wireless systems. The typical multi-user scenario, where several users access the same medium and the same resources to perform communication, requires powerful and efficient broadband transmission techniques that enable the utilization of the spectrum resources with very high efficiency. *Orthogonal frequency division multiplexing* (OFDM) is a transmission technique that elegantly addresses this problem and is currently being considered as base technology for current and future wireless communication systems. Moreover, error correcting codes are indispensable elements to improve the overall capacity of communication systems.

In this paper, we present a novel multiple access technique that is based on OFDM and braided convolutional codes (BCCs) [1], denominated as *braided code division multiple access* (BCDMA) [2]. As we will discuss throughout this paper, the BCDMA scheme results in a concep-

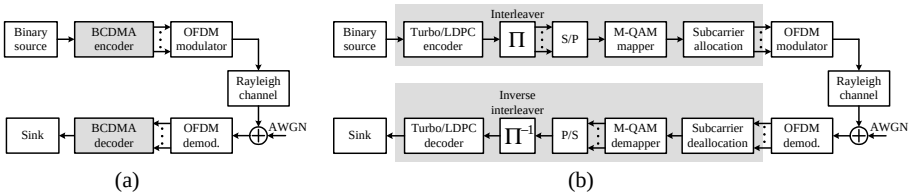

Figure 1. Systems under study. **(a)** BCDMA system. **(b)** Bit-interleaved coded modulation (BICM) system using turbo or LDPC codes.

tual change in the organization of modems for multiple access systems. This is due to the fact that error correction coding, interleaving for diversity exploitation, modulation and multiple access – which are generally processed by separate elements of a modem – are now concentrated in one single entity (as illustrated in Figure 1) that is derived from the typical two-dimensional array representation of the BCCs.

2. Braided Convolutional Codes

2.1 Encoders for BCCs

BCCs are asymptotically good, turbo-like codes that can be decoded by iterative application of the BCJR algorithm [1]. Like LDPC convolutional codes they can be decoded continuously with high-speed parallel pipeline architectures and are not limited to a fixed frame length. The implementation of a rate $R = 1/3$ BCC encoder, consisting of two rate $R_{\mathrm{cc}} = 2/3$ component convolutional encoders, is illustrated in Figure 2(a). Characteristic for BCCs is the feedback of each parity symbol to the input of the respective other component encoder, which makes them similar to generalized LDPC codes and results in good error correction properties. Asymptotically, their free distance grows linarly with their constraint length and the bit error probability converges at least doubly exponentially to zero with decoding iterations [1] [3]. The *multiple convolutional permutors* (MCPs) [4] $\mathbf{P}^{(0)}$, $\mathbf{P}^{(1)}$ and $\mathbf{P}^{(2)}$ are fundamental elements in the construction. An MCP of multiplicity Γ is defined as an infinite diagonal-type binary matrix with a fixed number Γ of 1's in every row and column and 0's elsewhere. The width w of an MCP is defined as the maximal number of columns spanned by the non-zero elements within a row. An example of an MCP, applied to an input sequence $\mathbf{u} = (u_0, u_1, \dots)$, is given in Figure 2(b).

The corresponding relation between the encoded symbols is conveniently described in a two-dimensional memory array, illustrated for $\Gamma = 5$ and $w = 10$ in Figure 3. The array is separated into three regions $\mathbb{P}^{(0)}$, $\mathbb{P}^{(1)}$ and $[\mathbb{P}^{(2)}]^{\mathrm{T}}$ corresponding to the different MCPs. The white cells are used to store the individual code symbols and their po-

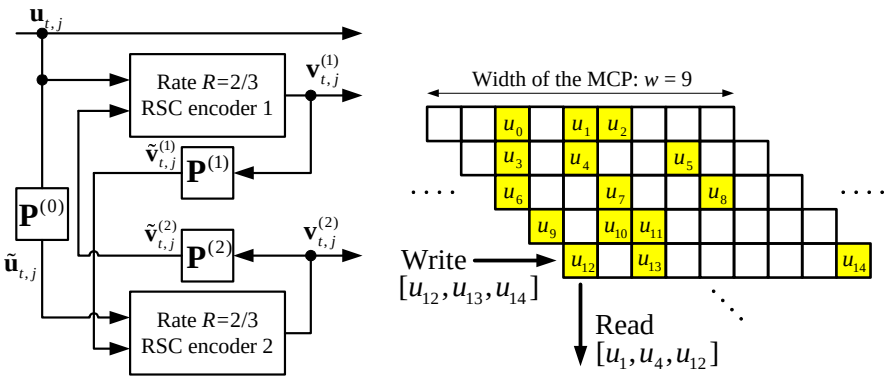

Figure 2. (a) Encoder for rate $R = 1/3$ braided convolutional codes. (b) Example of an MCP with $\Gamma = 3$.

sitions are specified by the non-zero entries of the MCPs. The encoding is performed as follows. At time instant t, the information symbols $\mathbf{U}_t = (\mathbf{u}_{t,0}, \cdots, \mathbf{u}_{t,\Gamma-1})$ enter the BCC encoder and are stored in their corresponding positions in row t of $\mathbb{P}^{(0)}$. The horizontal encoder operates in this row and uses the pairs of symbols $(\mathbf{u}_{t,j}, \tilde{\mathbf{v}}^{(2)}_{t,j})$, $j = 0, \cdots, \Gamma - 1$, from regions $[\mathbb{P}^{(2)}]^{\mathrm{T}}$ and $\mathbb{P}^{(0)}$, respectively, to produce new parity symbols $\mathbf{V}^{(1)}_t = (\mathbf{v}^{(1)}_{t,0}, \cdots, \mathbf{v}^{(1)}_{t,\Gamma-1})$ to be stored in region $\mathbb{P}^{(1)}$. The symbols $\tilde{\mathbf{v}}^{(2)}_{t,j}$ are parity symbols that earlier were produced by the vertical decoder and stored in row t of the array. The vertical encoder operates analogously in column t and uses symbol pairs $(\tilde{\mathbf{u}}_{t,j}, \tilde{\mathbf{v}}^{(1)}_{t,j})$ to produce new parity symbols $\mathbf{V}^{(2)}_t = (\mathbf{v}^{(2)}_{t,0}, \cdots, \mathbf{v}^{(2)}_{t,\Gamma-1})$. The output of the BCC encoder at time t is the vector of symbols $\mathbf{V}_t = (\mathbf{V}^{(2)}_t, \mathbf{U}_t, \mathbf{V}^{(1)}_t)$, whose positions are indicated by the dashed box in Figure 3.

2.2 BCCs and M-ary Modulation Schemes

BCCs are essentially binary codes. However, we can use the array representation of the BCCs also to encode symbols of M-ary modulation schemes. In this case, each used cell of the memory array will store $q = \log_2(M)$ bits. In other words, the symbols $\mathbf{u}_{t,j}$, $\tilde{\mathbf{u}}_{t,j}$, $\mathbf{v}^{(1)}_{t,j}$, $\tilde{\mathbf{v}}^{(1)}_{t,j}$, $\mathbf{v}^{(2)}_{t,j}$ and $\tilde{\mathbf{v}}^{(2)}_{t,j}$ will be binary vectors of length q. The encoding is then performed similar to the binary case, however, each parity symbol is obtained by encoding the q bits of each input symbol sequentially. For instance, in order to obtain the parity symbols $\mathbf{v}^{(1)}_{t,j} = (v^{(1)}_{t,j,0}, \cdots, v^{(1)}_{t,j,q-1})$ from the symbols $\mathbf{u}_{t,j} = (u_{t,j,0}, \cdots, u_{t,j,q-1})$ and $\tilde{\mathbf{v}}^{(2)}_{t,j} = (\tilde{v}^{(2)}_{t,j,0}, \cdots, \tilde{v}^{(2)}_{t,j,q-1})$,

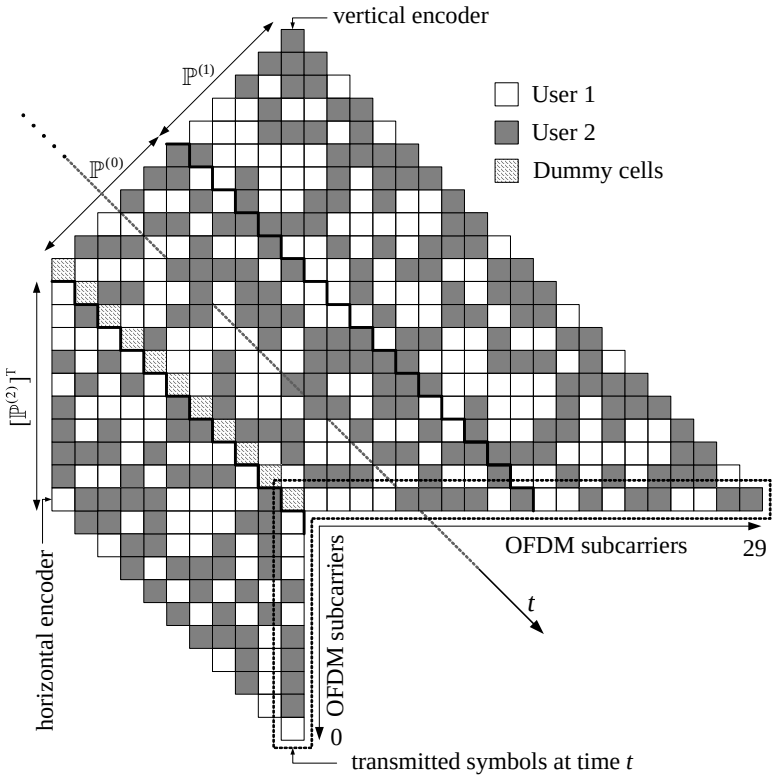

Figure 3. Array representation of BCDMA with two users.

the bits $u_{t,j,l}$ and $\tilde{v}^{(2)}_{t,j,l}$ enter the rate $R = 2/3$ component convolutional encoder to produce the bit $v^{(1)}_{t,j,l}$ for $l = 0$ to $q - 1$.

2.3 Decoders for BCCs

The BCCs can be decoded with a pipelined decoder architecture that enables continuous, high-speed decoding. As it can be observed in Figure 4, the main characteristic of this kind of decoder is the fact that all I decoding iterations can be performed in parallel by $2I$ concatenated identical *processors* $\mathcal{D}^{(e)}_i$, where $i = 1, \cdots, I$ and $e = 1, 2$. Thus, after an initial decoding delay, the estimated values for the code symbols are output by the pipeline decoder at each processing cycle in a continuous manner. For the particular case of BCCs, the $2I$ parallel processors are implementing an *windowed* version of the BCJR algorithm [5, 6]. In this case, each processor operates in a finite window of length W and calculates the *a posteriori probabilities* (APP) of all code symbols (i.e., information and parity symbols).

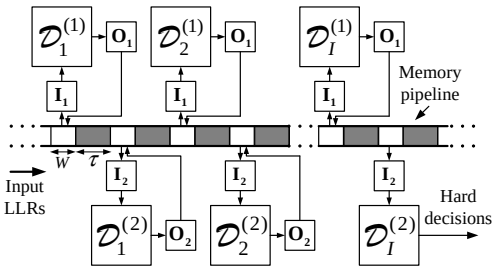

Figure 4. Pipeline decoder for BCCs.

More specifically, the decoding of BCCs using the pipeline decoder occurs as follows. At the t-th time instant, a vector of *log-likelihood ratios* (LLRs) $\mathbf{R}_t$ corresponding to the vector of code symbols $\mathbf{V}_t$ enters the memory pipeline as *a priori* information. Then, the *read-logic* $\mathbf{I}_1$ transfers the necessary data from the memory pipeline to the horizontal component code decoder $\mathcal{D}_1^{(1)}$. On its turn, the processor $\mathcal{D}_1^{(1)}$ performs the windowed BCJR decoding on the data and transfer the obtained extrinsic LLRs to the memory pipeline through the *write-logic* $\mathbf{O}_1$. Here, $\mathbf{I}_i$ and $\mathbf{O}_i$, with $i \in \{1, 2\}$, are determined by the MCPs $\mathbf{P}^{(0)}$, $\mathbf{P}^{(1)}$ and $\mathbf{P}^{(2)}$. After this, the processor $\mathcal{D}_1^{(1)}$ starts processing new data. Observe in Figure 4 that the current memory region used by $\mathcal{D}_1^{(1)}$ is separated from the vertical decoder $\mathcal{D}_1^{(2)}$ by τ positions. This is to avoid that different decoders operate in overlapping sets of coded bits at the same time. When the extrinsic LLRs produced by $\mathcal{D}_1^{(1)}$ reaches the decoder $\mathcal{D}_1^{(2)}$, vertical decoding is performed using the extrinsic LLRs produced by $\mathcal{D}_1^{(1)}$ as *a priori* information. The new extrinsic LLRs obtained by $\mathcal{D}_1^{(2)}$ are written into the memory pipeline and $\mathcal{D}_1^{(2)}$ starts to process new data. This process repeats through all horizontal and vertical processors until the data reaches the vertical decoder $\mathcal{D}_I^{(2)}$. This last processor outputs the final LLRs and hard decision is done to determine the values of the decoded bits.

3. Braided Code Division Multiple Access

In addition to the array representation of a BCC encoder, the example shown in Figure 3 can also be interpreted as the *subcarrier allocation pattern* of a BCDMA system for two users. In this case, we map each of the array cells at time t (i.e., cells inside the dashed box) to a subcarrier of an OFDM system. For instance, the BCDMA scheme depicted in Figure 3 would need as basis for its realization an OFDM system with at least $N_{\text{OFDM}} = 30$ subcarriers. We assume that the white cells are

associated with User 1 and gray cells are associated with User 2. The striped cells are dummy cells, they do not contain any information. If we number the OFDM subcarriers from the left to right, the symbols $\mathbb{S}_1(t) = \{\mathbf{v}_{t,0}^{(2)}, \mathbf{v}_{t,1}^{(2)}, \ldots, \mathbf{v}_{t,4}^{(2)}, \mathbf{u}_{t,0}, \mathbf{u}_{t,1}, \ldots, \mathbf{u}_{t,4}, \mathbf{v}_{t,0}^{(1)}, \mathbf{v}_{t,1}^{(1)}, \ldots, \mathbf{v}_{t,4}^{(1)}\}$, transmitted by User 1 at time instant t, will be mapped to the OFDM subcarriers $\mathbb{C}_1(t) = \{0, 5, 7, 8, 9, 10, 11, 12, 13, 18, 20, 21, 23, 26, 27\}$. Accordingly, the symbols $\mathbb{S}_2(t)$ of User 2 at time t will be mapped to the subcarriers $\mathbb{C}_2(t) = \{1, 2, 3, 4, 6, 14, 15, 16, 17, 19, 22, 24, 25, 28, 29\}$.

We can observe that the MCPs are the key components of our construction. They are responsible for defining the BCCs, as well as, the subcarrier allocation pattern of the users. In Figure 3, $\mathbb{P}^{(0)}$, $\mathbb{P}^{(1)}$ and $[\mathbb{P}^{(2)}]^{\mathrm{T}}$ denote the sets containing the MCPs $\mathbf{P}_k^{(i)}$, $i \in \{0, 1, 2\}$, $k \in \{0, \cdots, K-1\}$, of the $K = 2$ users of the system. The generalization for $K \geq 3$ is straightforward. However, a fundamental condition that the sets $\mathbb{P}^{(i)}$, $i \in \{0, 1, 2\}$, must fulfill in order to define a BCDMA system is that their elements must be orthogonal to each other. Considering the definition of an MCP, this orthogonality condition can be formulated as

$$p_{t,t'}^{(i),k_1} \cdot p_{t,t'}^{(i),k_2} = 0, \ \forall t, t' \in \mathbb{Z}^+ \text{ and } k_1 \neq k_2, \tag{1}$$

where $p_{t,t'}^{(i),k}$ is an element of the MCP $\mathbf{P}_k^{(i)}$, $i \in \{0, 1, 2\}$, associated with the k-th user of the system. This orthogonality condition implies that the different users of the BCDMA system do not share OFDM subcarriers to transmit their symbols at the time instant t. As a consequence, they do not cause interference to each other.

3.1 Spectrum Management for BCDMA Systems

In spite of having the subcarrier allocation pattern determined by the error control coding scheme, the BCDMA system is still very flexible concerning the spectrum management for the several users. Considering that the available spectrum is given by the number of OFDM subcarriers N_{OFDM}, some straightforward strategies for spectrum management are listed below:

a) If $\lfloor N_{\mathrm{OFDM}}/3w \rfloor < 2$ the throughput of the users can increased or reduced by increasing or reducing the multiplicities Γ, respectively. Alternatively, different rows of the MCPs can be overlapped into a single OFDM symbol to increase the throughput, or the elements of the rows of the MCPs can be spread across different OFDM symbols to decrease the throughput.

b) If $\lfloor N_{\mathrm{OFDM}}/3w \rfloor \geq 2$ the above mentioned techniques can also be applied. In addition, different rows of the MCPs can be placed into orthogonal sub-bands of a single OFDM symbol to increase the throughput.

Observe that by applying the spectrum managements techniques from above, the orthogonality condition in (1) must be redefined.

3.2 Further Remarks

There are some points that are worth discussing when considering the constructions presented in this section. As we can observe in Figure 3, the sub-carriers belonging to a particular user are spread in frequency domain. This is a very important feature that enables the BCDMA system to exploit the *frequency diversity* of the channel. Another very important property that belongs the BCDMA system is the *frequency hopping* experienced by the users in the succession of the time instants, i.e., the subcarriers used by a particular user are different for the succession of time instants. This last property implies that good and also bad parts of the spectrum are equally (or almost equally) distributed among the users. In other words, it means that the BCDMA system is *fair*. Additionally, if BCDMA is supposed to be deployed in a cellular system with *frequency reuse*, the frequency hopping is very important for averaging the inter-cell interference.

4. Simulation Results

In this section, we evaluate the performance of the BCDMA system compared to *bit-interleaved coded modulation* (BICM) systems [7, 8] using turbo and LDPC codes.

For the BCDMA system, the component convolutional codes have rate $R = 2/3$ and 4 states. Their generator matrices are given by

$$\mathbf{G}(D) = \begin{pmatrix} 1 & 0 & 1/(1+D+D^2) \\ 0 & 1 & (1+D^2)/(1+D+D^2) \end{pmatrix}. \tag{2}$$

On the other hand, the component codes of the turbo code of the BICM system have rate $R = 1/2$ and also 4 states. Their generator matrices are given by

$$\mathbf{G}(D) = \begin{pmatrix} 1 & (1+D^2)/(1+D+D^2) \end{pmatrix}. \tag{3}$$

Moreover, the rate $R = 1/3$ LDPC code in our simulations is the one used in the DVB-S2 standard [9] and all MCPs, interleavers and the subcarrier allocation pattern of the BICM systems have been randomly generated.

In all systems, the underlying OFDM system consists of $N_{\mathrm{OFDM}} = 1024$ subcarriers and a *cyclic prefix* of length $N_{\mathrm{CP}} = 16$, which is appended to the beginning of each transmitted OFDM symbol. Additionally, we use a 10-path i.i.d. frequency selective Rayleigh fading channel in our simulations that is constant over the duration of one OFDM symbol but varies independently from symbol to symbol. Moreover, in the OFDM demodulators of the systems a linear MMSE equalizer with perfect channel knowledge is used to mitigate the channel distortions.

In our simulations, the BCDMA system was observed in two different configurations, which are listed below:

1. $w = 50$, $\Gamma = 5$, QPSK modulation, block length $L = 63800$ bits.

2. $w = 50$, $\Gamma = 5$, 16-QAM modulation, block length $L = 62800$ bits.

For the BCDMA configurations from above, the BCC encoders have been terminated with $2w\Gamma \log_2(M)$ zero bits, resulting in coding rates of $R \approx 0.323$ for QPSK and $R \approx 0.312$ for 16-QAM. Moreover, $N_{\mathrm{U}} = 90$ OFDM subcarriers are used in each OFDM symbol to transport user data.

The turbo coded BICM system has also been examined in different configurations. Here, an interleaver length of $N = 21600$ (resulting in terminated blocks of lengths $L = 64808$ and coding rate $R \approx 1/3$) has been combined with QPSK and 16-QAM modulations. The $R = 1/3$ LDPC code has length $L = 64800$ and has also been combined with QPSK and 16-QAM modulations. As in the case of the BCDMA system, the subcarrier allocation module of the BICM systems assigns $N_{\mathrm{U}} = 90$ subcarriers to user data in each OFDM symbol.

Figure 5 shows the BER performance of the BCDMA system compared against the BICM systems. As we can observe below error rates of 10^{-3}, the BCDMA system considerably outperforms the turbo coded BICM system, which shows its typical error floor behavior in the high SNR regime. In [2], we showed that the error floor phenomenon of a BICM turbo coded system was even more evident when linear least squares equalizers are used, while the BCDMA system is quite robust against the noise enhancement of such equalizes. Here, it is worth to mention that both systems have almost the same decoding complexity. However, the BCDMA system has much more steep BER curves as an indication of its good minimum distances properties. In Figure 5, we also have the BER curves for the LDPC coded BICM system. We can observe that the LDPC coded system outperforms the BCDMA system. At this point, however, we should be careful since LDPC codes of rates $R < 0.5$ are usually more complex than trellis decodable codes of similar rates [10]. Moreover, if we consider the interleaving complexity of the

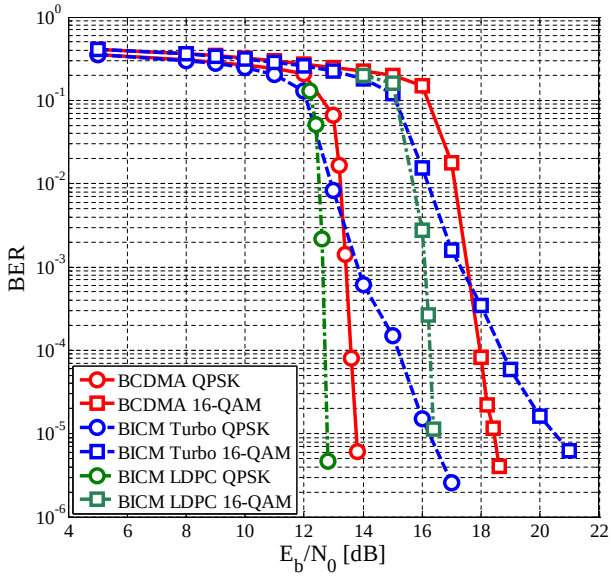

Figure 5. BER comparison of BCDMA and BICM systems.

systems in Figure 5, we can see that the BCDMA systems with $w = 50$, in comparison to $N = 21600$ and $L = 64800$ of the BICM systems, have much more local connections in their interleavers and are, therefore, much more suitable for low complexity hardware implementations.

5. Conclusions

In this paper, we presented the general principles of a novel multiple access scheme called *braided code division multiple access* (BCDMA). Aside from providing a flexible and efficient medium access scheme for a large number of users, the application of the BCDMA concept results in a conceptual change in the design of multiple access modems. In this case, processing tasks that are traditionally considered in separate (i.e., error correction coding, interleaving for diversity exploitation, modulation and multiple access) are now combined in one single entity. Moreover, the pipeline decoding of the underlying *braided convolutional codes* (BCCs) enables very high speed VLSI implementations. Simulation results have also shown that the BCDMA system is an attractive alternative to conventional systems based on bit-interleaved coded modulation.

We consider BCDMA to be a promising research topic. Several points regarding this new technique remain open. For instance, the design of the MCPs to simultaneously maximize the error correction capabilities of the underlying BCC, frequency diversity exploitation, fairness and interference averaging property must be studied. In addition, some other

issues like decoding delay reduction, VLSI implementation, rate compatibility, synchronization and channel estimation are also very interesting. Finally, we conjecture that the gap to the LDPC coded system can be reduced by proper choice of the component codes, as well as, optimization of the bit mapping scheme used in the M-ary modulations. This is our current research focus.

Acknowledgment

The authors are grateful for the use of the high performance computing facilities of the ZIH at the TU Dresden.

References

[1] W. Zhang, , M. Lentmaier, K.Sh. Zigangirov, and D.J. Costello, Jr. Braided convolutional codes: a new class of turbo-like codes. *IEEE Trans. Inform. Theory.* submitted for publication.

[2] M.B.S. Tavares, M. Lentmaier, K. Sh. Zigangirov, and G.P. Fettweis. New multi-user OFDM scheme: Braided code division multiple access. In *Proc. Asilomar Conference on Signals, Systems and Computers*, Pacific Grove, CA, Oct. 2008.

[3] M.B.S. Tavares, M. Lentmaier, G.P. Fettweis, and K.Sh. Zigangirov. Asymptotic distance and convergence analysis of braided protograph convolutional codes. In *Proceedings of the 46th Annual Allerton Conference on Communication, Control, and Computing*, Monticello, IL, September 2008.

[4] A. Jiménez Feltström, M. Lentmaier, D.V. Truhachev, and K.Sh. Zigangirov. Braided block codes. *IEEE Trans. Inform. Theory.* accepted for publication.

[5] S. Benedetto, G. Montorsi, D. Divsalar, and F. Pollara. A soft-input soft-output maximum a posteriori (MAP) module to decode parallel and serial concatenated codes. *JPL TDA Progress Report*, 42(127):1–20, November 1996.

[6] A.J. Viterbi. An intuitive justification of the MAP decoder for convolutional codes. *IEEE J. Select. Areas Commun.*, 16(2):260–264, February 1998.

[7] E. Zehavi. 8-PSK trellis codes for a Rayleigh channel. *IEEE Trans. Commun.*, 40(5):873–884, May 1992.

[8] G. Caire, G. Taricco, and E. Biglieri. Bit-interleaved coded modulation. *IEEE Trans. Inform. Theory*, 44(3):927–946, May 1998.

[9] *European Telecommunications Standards Institute (ETSI). Digital Video Broadcasting (DVB); Second generation framing structure, channel coding and modulation systems for Broadcasting, Interactive Services, News Gathering and other broadband satellite applications; EN 302 307 V1.1.1 (2004-06).*

[10] K.S. Andrews, D. Divsalar, S. Dolinar, J. Hamkins, C.R. Jones, and F. Pollara. The development of turbo and LDPC codes for deep-space applications. *Proc. IEEE*, 95(11):2142–2156, November 2007.